Ethylene Polymerization, On-Line Particle Growth Monitoring, and in Situ Nanocomposite Formation Using Catalysts Supported on Arylsulfonic Acid-Modified Boehmites

Rainer Xalter, Frédéric Pelascini, and Rolf Mülhaupt*

Freiburg Materials Research Center and Institute for Macromolecular Chemistry, Albert-Ludwigs University Freiburg, Stefan-Meier-Str. 31, D-79104 Freiburg, Germany

Received November 26, 2007; Revised Manuscript Received February 12, 2008

ABSTRACT: Ethylene was polymerized on Cp_2ZrCl_2 activated by methylalumoxane (MAO) supported on boehmites modified with arylsulfonic acids. In comparison with unmodified boehmites, boehmites modified with arylsulfonic acids gave significantly higher MAO uptakes. Cp_2ZrCl_2 activated with arylsulfonic acid-modified boehmites/MAO gave notably higher catalyst activities compared with those of homogeneous Cp_2ZrCl_2/MAO and Cp_2ZrCl_2 activated with unmodified boehmite/MAO and SiO_2/MAO. According to ^{13}C CP-MAS NMR investigations of MAO supported on *p*-toluenesulfonic acid-modified boehmite, partial alkylation of *p*-toluenesulfonate by MAO accounted for the formation of methyl *p*-tolyl sulfone as an electron-donating catalyst modifier. Polymer particle morphologies and size distributions were examined off-line by means of scanning electron microscopy, light scattering on dry powder dispersions, and CCD-mediated powder particle image analysis. The mechanism of polymer particle formation via deagglomeration of boehmite particles was elucidated by means of on-line monitoring using focused beam reflectance measurement. As evidenced by transmission electron microscopy, polyethylene particles contained uniformly dispersed boehmite crystallite aggregates with average diameters of 100 nm.

Introduction

The development of supported olefin polymerization catalysts represents an important step toward industrial applications of single site catalysts such as alumoxane-activated metallocenes and postmetallocenes. It is well-known that the heterogenization[1,2] of homogeneous olefin polymerization catalysts prevents reactor fouling and is a prerequisite for good product morphology and high polymer bulk density. Since the discovery of methylalumoxane (MAO) by Sinn and Kaminsky[3,4] and the development of stereospecific *ansa*-metallocene catalysts by Brintzinger,[5,6] a wide range of materials has been evaluated for supporting single site catalysts. These include silica, alumina, zeolites, clays, and magnesium chloride[1] as well as organic carriers such as starch,[7] cyclodextrins,[8,9] synthetic polymer microparticles,[2] and modified polystyrene nanoparticles.[10−12]

Much less is known concerning the preparation of heterogenized metallocene catalysts using boehmite (AlO(OH)) as support material. To the best of our knowledge, boehmite was employed for the first time by Kissin who utilized AlO(OH) and $Al(OH)_3$ for the in situ formation of MAO by reaction with trimethylaluminum (TMA).[13] Collins and co-workers[14] employed commercial boehmite as a precursor in order to produce an ultrapure alumina support by means of calcination. Recently, Marques and De Alcantara[15] described ethylene polymerization metallocene catalysts supported on thermally and chemically treated boehmites. After treating boehmite with TMA or NaOH, the heterogeneous catalyst systems afforded activities comparable to those of the homogeneous precursor, while sintering at 550 °C (conversion to γ-alumina) prior to chemical treatments resulted in inferior catalyst activity. Barron and co-workers[16] used *p*-hydroxybenzoic acid-modified boehmite nanoparticles as support for MAO. At elevated temperatures, the phenolic group of *p*-hydroxybenzoate reacted with MAO to produce carboxylate-alumoxane nanoparticles with covalent attachment of MAO onto the boehmite nanoparticles. An active polymerization catalyst was obtained by impregnation of the MAO-treated carboxylate-alumoxane with Cp_2ZrCl_2. For short polymerization times, the supported catalyst showed an activity slightly higher than that of the corresponding homogeneous catalyst. However, catalyst activity dropped off quickly and was lost entirely after 60 min due to rapid catalyst deactivation.

Here, we report on the use of arylsulfonic acid-modified boehmites, prepared by a sol−gel process. Such organophilic boehmites are known to consist of agglomerates of nanometer-scaled boehmite crystallites which deagglomerate in organic solvents to form stable boehmite dispersions. Such boehmite nanoparticle dispersions have been utilized as support for MAO and for the in situ activation of metallocene. The objective of this research has been to examine ethylene polymerization and polyethylene morphology development as a function of the boehmite surface modification and the catalyst preparation methods as well as the polymerization conditions. Another objective has been to exploit the catalyst fragmentation of boehmite supports during ethylene polymerization in order to in situ produce nanocomposites. Polymer particle growth has been monitored by means of on-line focused laser beam reflectance measurement (FBRM) during ethylene slurry polymerization in a stirred reactor.

Experimental Section

Materials. Cp_2ZrCl_2 (98%) was purchased from Aldrich, MAO as a 10 wt % solution in toluene from Crompton GmbH, Bergkamen, *n*-heptane and toluene from Merck, and ethylene from Messer-Griesheim. Disperal samples were generously provided by Sasol Germany, Hamburg. They are generally synthesized by means of a sol–gel process starting from aluminum alkoxides, followed by controlled crystallization and spray drying.[17,18] Silica gel Sylopol 948 was obtained from Grace Davison. Cp_2ZrCl_2, MAO, and ethylene were used without further purification. Solvents were dried by refluxing over Na/K alloy under inert gas and distilled prior to use. Disperal samples were dried in a vacuum at 100 °C for 2 h, and Sylopol 948 was dried in a vacuum at 150 °C for 2.5 h. All manipulations were carried out under an argon atmosphere by standard Schlenk, vacuum, and glovebox techniques.

* Corresponding author.

10.1021/ma702623e CCC: $40.75
Published on Web 04/10/2008

Catalyst Characterization. The amount of MAO supported on the carrier was determined for all particles used gravimetrically, i.e., by the weight increase after MAO treatment according to the above-mentioned catalyst preparation. Therefore, particles were dried under vacuum after having been washed with *n*-heptane. Solid-state ^{13}C CP-MAS NMR spectra were recorded at 75 MHz on a Bruker Avance 300 spectrometer using spinning rates of 9–10.5 kHz. FT-IR spectra were recorded on a Bruker Vector 22 spectrometer. FT-IR samples of dried OS1, solid MAO, and MAO-treated OS1 were prepared as Nujol mull between NaCl plates in a glovebox.

Polymer Characterization. Molecular weights and molecular weight distributions of the polymers were determined by size exclusion chromatography using a PL-220 chromatograph (Polymer Laboratories) at 140 °C equipped with 3 PLGel mixed-bed columns. The solvent used was 1,2,4-trichlorobenzene, stabilized with 2 mg/mL Irganox 1010, at a flow rate of 1 mL/min. PS standards with narrow molecular weight distributions were used for calibration; the molecular weights given are referred to PS. Differential scanning calorimetry measurements were carried out on a Seiko 6200 thermal analysis system in the temperature range from −70 to 170 °C at a heating rate of 10 K/min. The second heating curve was used for evaluation. Thermogravimetric analysis was performed on a Netzsch STA-409 instrument under a nitrogen atmosphere and in air, respectively. For environmental scanning electron microscopy (ESEM), samples were sputtered with Au/Pd in a Pollaron Sputter Coater SC 7640 (deposit thickness ca. 30 nm). ESEM images were recorded with an ESEM 2020, Electroscan, Wilmington, MA, U.S.A., in a water vapor atmosphere (5 Torr) at an acceleration voltage of 25 kV. Secondary electrons were detected by a gaseous secondary electron detector. Transmission electron microscopy (TEM) measurements were carried out on a LEO 912 Omega instrument applying an acceleration voltage of 120 keV. The specimens were prepared by melting the polymer particles and subsequently cutting the resulting films in an ultramicrotome (Leica Ultracut UCT) equipped with a cryochamber (Leica EM FCS). Thin sections of about 50 nm were cut with a Diatome diamond knife at −120 °C. Particle size distribution measurements were performed by light scattering experiments under dry dispersion conditions using a Horiba LA-920 instrument equipped with a dry dispersion system. In addition, particle size distributions of polymer particles were measured using a Retsch Camsizer, which employs two CCD cameras with different resolutions and image analysis software. On-line measurements of chord length distributions were performed using a Lasentec FBRM D600VL probe applying a scanning speed of 2 m/s and a measurement interval of 2 s.

Catalyst Preparation. In a typical experiment, 0.50 g of the predried support was stirred in 8.5 mL of a 10 wt % MAO solution at room temperature for 30 min. After sedimentation, the supernatant liquid was removed with a pipet. The solid was then washed two times with 10 mL of *n*-heptane by slurring the particles for 1 min. Subsequently, the support was impregnated with the catalyst by the addition of the desired amount of a Cp_2ZrCl_2 solution in toluene (1 mg/mL) and stirring for 5 min. This suspension was taken up in 20 mL of *n*-heptane and injected into the polymerization reactor (reaction type "in situ immobilization"). In a modification of this procedure, the supernatant impregnation solution was removed, and the catalyst particles were dried under vacuum, until a free-flowing powder was obtained. The desired amount of the catalyst was then dispersed in 20 mL of *n*-heptane for injection into the reactor (reaction type "dry catalyst").

Ethylene Polymerizations. Pretests were performed in a 200 mL Büchi Miniclave glass reactor equipped with a mechanical stirrer. For these experiments, 120 mg of each support was treated with 1.5 mL MAO solution and 1 mL of a Cp_2ZrCl_2 solution in toluene (1 mg/mL) according to the above-mentioned procedure without drying the final catalyst particles. The resultant catalyst slurry was taken up in 20 mL *n*-heptane and injected into the reactor filled with *n*-heptane so that the total volume of the reaction mixture was 70 mL. The polymerization was started by applying 3 bar overpressure of ethylene, and the reactor temperature was kept constant at 20 °C by means of a water bath. After a polymerization time of 15 min, the reaction was stopped by venting the reactor. The polymer was precipitated in a 300 mL volume of methanol acidified with 10 mL of 15 wt % HCl and dried at 60 °C under vacuum.

Scheme 1. Structures of Arylsulfonic Acid-Modified Boehmites OS1 and OS2

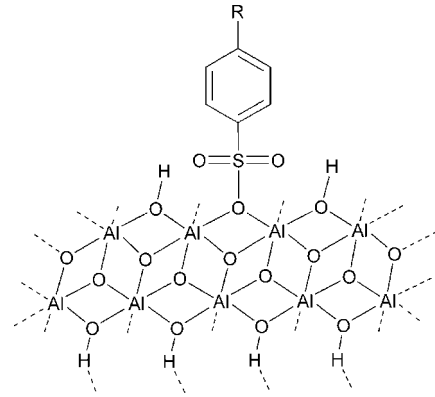

Larger-scale polymerizations were carried out in a semiautomated 1.0 L double-jacket metal reactor. Important parameters such as reactor temperature, stirrer rotation speed, and ethylene pressure were controlled and recorded by a computer. The reactor was filled with *n*-heptane and flushed with ethylene until the solvent was saturated. The reaction was started by the addition of the catalyst particles suspended in a 20 mL volume of *n*-heptane. The ethylene pressure was kept constant at 3 bar during the polymerization by means of a mass flow meter. The total volume of the reaction mixture was 500 mL. The polymer particles formed were filtered off and dried at 60 °C under vacuum.

Results and Discussion

Role of Boehmite Modification. In addition to a nonfunctionalized boehmite (D20) consisting of large agglomerates of boehmite crystallites with 20 nm average crystallite size, *p*-toluenesulfonic acid-modified boehmite (OS1), and *p*-(C_{10}−C_{13})-alkyl benzenesulfonic acid-modified boehmite (OS2) with crystallite sizes of 10–12 nm were employed as supports for MAO. The resulting MAO/boehmite particles were subsequently used for the in situ activation of Cp_2ZrCl_2. The structures of pure boehmite as well as of the arylsulfonic acid-modified boehmites OS1 and OS2 are displayed in Scheme 1. Catalyst activities were characterized and compared to those of the homogeneous catalyst Cp_2ZrCl_2/MAO and conventional SiO_2/MAO-activated Cp_2ZrCl_2 prepared according to the same procedure.

The properties of the tested support materials are listed in Table 1. Pure boehmite D20 is dispersible in acidified water, whereas the *p*-toluenesulfonic acid modification renders boehmite OS1 organophilic and thus enables the deagglomeration and formation of stable nanoboehmite dispersions in many polar organic solvents such as alcohols. The use of benzenesulfonic acid substituted with (C_{10}−C_{13})-alkyl chains in para position (OS2) improves organophilicity and affords nanoboehmite dispersions in most organic solvents including less polar solvents such as toluene.

MAO was supported on modified and unmodified boehmite particles by suspending them in a 10 wt % MAO solution in toluene for 30 min, followed by washing with *n*-heptane. The reaction is moderately exothermic, and gas evolution is observed during the first few minutes for all supports. The reaction between particles and MAO did not require elevated tempera-

Table 1. Properties of Support Materials[a]

	Disperal 20	Disperal OS1	Disperal OS2	Sylopol 948
sample code	D20	OS1	OS2	SiO_2
crystallite size [nm]	20	10	12	n/a
surface area[b] [m^2/g]	150	200	230	298
pore volume[b] [mL/g]	0.7	0.5	0.5	1.65
mean particle size[c] [μm]	41	134	27	62
surface modification	none	*p*-TosOH[d]	*p*-R(C_6H_4)SO_3H[e]	n/a
modifier [wt %]	n/a	7	12	n/a
modifier [mmol/g boehmite]	n/a	0.44	0.39	n/a

[a] Data provided by manufacturer, if not indicated differently. [b] Measured by N_2 adsorption; Disperal samples were calcined at 550 °C for 3 h prior to measurement. [c] Measurements performed in our laboratory on a Horiba LA-920 particle size analyzer under dry dispersion conditions. [d] Modifier: *p*-toluenesulfonic acid. [e] Modifier: *p*-alkyl benzenesulfonic acid (R = C_nH_{2n+1} with n = 10–13; mixture of isomers).

Table 2. MAO Uptake of Boehmites, Catalyst Activities, and Properties of Polyethylene Obtained with Boehmite/MAO-Activated Cp_2ZrCl_2

run	support	MAO content [mmol Al_{MAO}/g support]	Al/Zr	activity[a] [kg_{PE}/mol_{Zr} × h]	T_m [°C]	X[b] [%]	filler content [wt %]
A1	D20	1.4	100	2150	134	59	12.8
A2	OS1	12.1	830	4230	135	59	6.5
A3	OS2	5.7	400	4890	136	60	5.7
A4	SiO_2	5.7	400	1690	136	58	16.60
A5	homogeneous		1500	2780	136	53	

[a] Polymerization conditions: 1.7 μmol Cp_2ZrCl_2, 120 mg support, 70 mL *n*-heptane, 20 °C, 3 bar ethylene, 15 min. [b] Degree of crystallinity, calculated on the basis of a melt enthalpy of 290 mJ/mg for perfectly crystalline polyethylene (PE).[19]

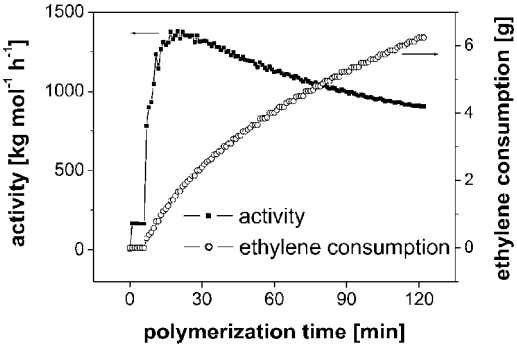

Figure 1. Kinetic analysis of ethylene polymerization on Cp_2ZrCl_2/MAO/OS1 (run B1 in Table 3).

Table 3. Catalytic Activities of Cp_2ZrCl_2/MAO/S1 and Polyethylene Properties as a Function of Catalyst Preparation Method and Polymerization Temperature

run	T_{react} [°C]	catalyst preparation	activity[a] [kg_{PE}/mol_{Zr} × h]	M_w [10^3 g/mol]	M_w/M_n	filler content [wt %]
B1	25	in situ immob	870	n.d.	n.d.	3.4
B2	25	dry powder	690	459	2.6	4.3
B3	40	dry powder	990	400	2.9	3.0
B4	50	dry powder	1190	270	3.9	2.4
B5	75	dry powder	650	162	4.4	4.5

[a] Polymerization conditions: 4.3 μmol Cp_2ZrCl_2, 250 mg OS1, Al/Zr = 700, 500 mL *n*-heptane, 3 bar ethylene, 120 min.

tures, but appeared to be very fast even at ambient temperature. In contrast, the *p*-hydroxybenzoic acid-modified boehmite nanoparticle support, described by Barron and co-workers,[16] required refluxing for 24 h in order to achieve covalent MAO attachment.

The MAO uptake values of all MAO-treated support samples, as determined gravimetrically after stirring for 30 min at room temperature and drying in vacuum, are summarized in Table 2. OS1 gave 8-fold MAO uptake, followed by OS2 with 4-fold MAO uptake with respect to that of the unmodified boehmite D20. OS1/MAO contained 41 wt % of MAO, whereas the MAO content of D20/MAO was only 8 wt %. The MAO uptake of SiO_2 was very similar to that of OS2. It is noteworthy that the maximum amount of MAO immobilized on OS1 was found to be independent of heterogenization time, temperature, and the solvent used for washing. Prolonged treatment at elevated temperatures and washing with toluene led to the same results as obtained when using the standard conditions outlined above.

Since the surface area and pore volume of all tested boehmites are similar to each other, the electron-donor function of the arylsulfonates on the modified boehmites toward Lewis-acidic MAO is likely to account for the large MAO uptake by the modified boehmites. In addition, the higher organophilicity of the modified boehmites might also enhance the MAO load due to better wetting of the supports by the MAO solution. The lower MAO uptake of OS2 with respect to that of OS1 is likely to result from reduced Lewis acid/Lewis base interactions due to the steric hindrance of the long alkyl chains of the *p*-(C_{10}−C_{13})-alkyl benzenesulfonate.

Polymerization was performed by in situ activation of Cp_2ZrCl_2 with different MAO/boehmite supports in order to examine the role of boemite modification. Procedures for the in situ activation were similar to those proposed by Soares and co-workers.[20,21] Typically, the MAO-treated boehmite particles were impregnated with a solution of Cp_2ZrCl_2 in toluene for 5 min, and the resulting suspension was immediately transferred into the polymerization reactor. To avoid leaching of the activated catalyst, *n*-heptane was chosen as the polymerization medium. For all types of Cp_2ZrCl_2/MAO/boehmite catalysts, no reactor fouling was observed. This indicates that leaching was not an issue with these boehmite supports. It is important to note that for OS1 and OS2, the 2-fold catalyst activities were obtained with respect to the homogeneous Cp_2ZrCl_2/MAO catalyst while at the same time the activator demand was much lower. It is noteworthy that, in contrast to these results, most heterogenized metallocene catalysts give significantly lower activities compared with those of their corresponding homogeneous counterparts.[1] With respect to the Cp_2ZrCl_2/MAO/SiO_2 catalyst, Cp_2ZrCl_2 activated by MAO/OS1 and MAO/OS2 gave 3-fold activities. Interestingly, the activity of Cp_2ZrCl_2 supported on the highly organophilic boehmite OS2 exceeds the activity obtained when using OS1 as support, though the MAO load is much lower on OS2 compared with that of OS1. Possibly the long alkyl chains of the *p*-(C_{10}−C_{13})-alkyl benzenesulfonate modification of OS2 shield the support surface more efficiently than the *p*-toluenesulfonate groups of OS1, thus protecting the catalyst centers from being deactivated by surface hydroxyl groups.

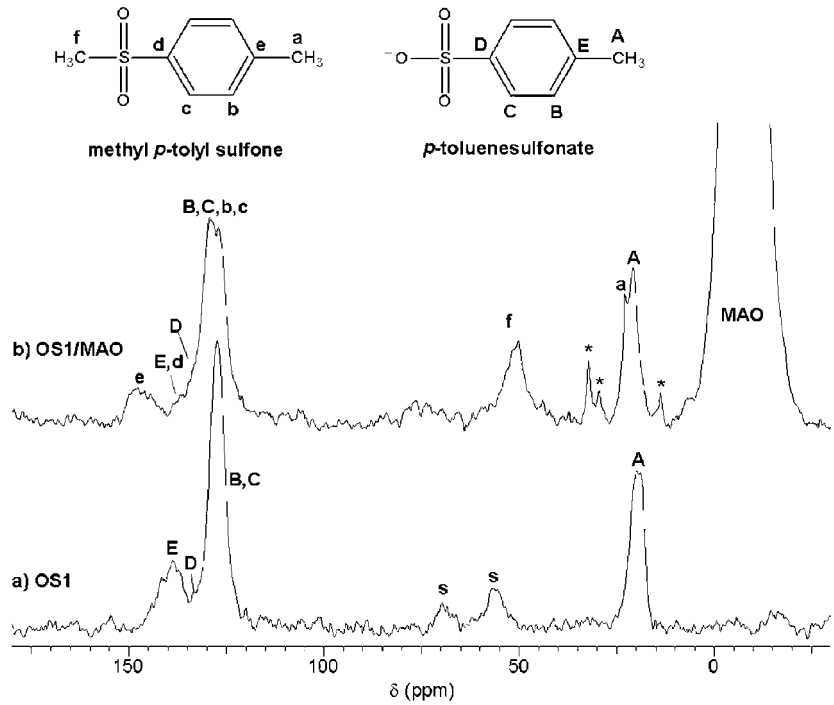

Figure 2. ^{13}C CP-MAS spectra of (a) OS1 and (b) OS1/MAO; signals marked with an asterisk correspond to *n*-heptane residues, and *s* denotes satellite signals.

Investigation of Cp_2ZrCl_2 Activated by MAO/*p*-Toluenesulfonic Acid-Modified Boehmite. The polymerization rate/time function of ethylene polymerization catalyzed by Cp_2ZrCl_2/MAO/OS1 at 25 °C is displayed in Figure 1. The consumption of ethylene remained remarkably constant throughout the polymerization time of 120 min with only marginal losses of catalyst activity due to catalyst deactivation. When compared with the *p*-hydroxybenzoic acid-modified boehmite used by Barron and co-workers, who reported total deactivation of their catalyst system after 1 h,[16] arylsulfonic acid-modified boehmites and the MAO immobilization at ambient temperature afforded very stable catalysts useful in slurry and gas-phase polymerization.

As an alternative to the in situ activation, the Cp_2ZrCl_2/MAO/OS1 catalyst was washed and dried under vacuum to produce a free-flowing dry powder. This powder was redispersed in *n*-heptane before transferring it to the reactor. From Table 3 it is apparent that both the in situ activation and the injection of dried catalysts gave comparable activities. Optimum catalyst activity was found at 50 °C. This observation is in accord with reports by Do Couto and co-workers[22] who observed highest activity of the homogeneous catalyst Cp_2ZrCl_2/MAO at around 60 °C. Polyethylene molecular weights were found to decrease with increasing polymerization temperatures.

Interactions between MAO and *p*-Toluenesulfonic Acid-Modified Boehmite. The interactions between MAO and the *p*-toluenesulfonic acid-modified boehmite (OS1) were investigated by means of solid-state ^{13}C CP-MAS NMR. The spectra of OS1 and OS1/MAO are displayed in Figure 2. While for the *p*-toluenesulfonate groups of OS1 three signals are observable (20 ppm, CH_3; 127 ppm, *ipso*-, *ortho*-, and *meta*-C; 139 ppm, *para*-C), five additional signals appear in the spectrum of OS1/MAO. The broad intense signal at −8 ppm corresponds to the methyl groups of MAO, but there are also new signals at 23, 50, 129, and 148 ppm. This indicates the formation of methyl *p*-tolyl sulfone, generated by the alkylation of the sulfonate with either MAO or free TMA. The chemical shifts for methyl *p*-tolyl sulfone in $CDCl_3$ are 145 ppm for the para position, 138 ppm for the ipso position, 130 ppm for the ortho position, and 127 ppm for the meta position,[23] which are in good accordance with those of the obtained spectrum. The signal corresponding to the aromatic carbons of *p*-toluenesulfonate in the ipso, ortho, and meta positions appearing at 127 ppm is retained, whereas the new signal at 129 ppm can be ascribed to the ortho carbons of the newly formed methyl *p*-tolyl sulfone. However, an exact assignment of the individual signals contained in the broad signal with shifts ranging from 122 to 140 ppm is difficult. The signal recorded at 50 ppm can be assigned to the sulfone methyl group, which appears at 45 ppm in $CDCl_3$. This difference can be explained by strong Lewis donor–acceptor interactions of the sulfone group and MAO, causing a low-field shift as a result of reduced electron density at the sulfone methyl group. The peak appearing at 23 ppm, which is close to the peak of the toluene methyl group of *p*-toluenesulfonate, but slightly shifted downfield, probably corresponds to the methyl group of the sulfone. According to solution NMR results, essentially the same chemical shift would be expected for this toluene methyl group in both the sulfone and the sulfonate, but differences in the Lewis acid/Lewis base interactions with MAO are likely to account for the presence of the two separate peaks.

In conclusion, according to the ^{13}C CP-MAS NMR results, OS1/MAO appears to consist of *p*-toluenesulfonate bound to the particle surface and tethering MAO to the particles via Lewis acid/Lewis base interactions. In addition, methyl *p*-tolyl sulfone is present, which is tightly coordinated to MAO immobilized on the surface of the particles (cf. Scheme 2). It is not extracted with *n*-heptane. The resolution of the CP-MAS NMR spectra does not permit one to quantify the sulfone content, but the signal intensity of the sulfone indicates that substantial amounts of the sulfonate are converted into the sulfone.

Off-Line Monitoring of Polyethylene Morphology. The morphology development of polyethylene particles was monitored off-line by using environmental scanning electron microscopy (ESEM), transmission electron microscopy (TEM), light scattering (LS) on dry particle dispersions, and CCD camera-mediated powder particle image analysis. A typical

Scheme 2. Schematic Representation of the Interaction of MAO with *p*-Toluenesulfonic Acid-Modified Boehmite

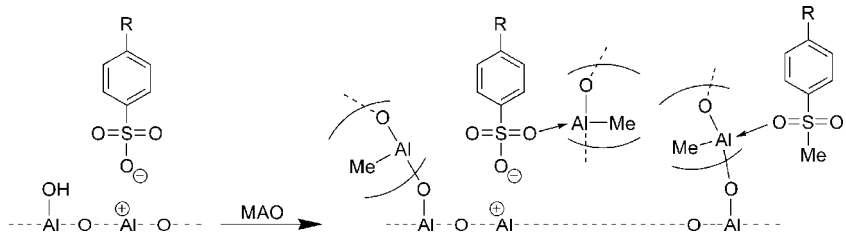

ESEM image is displayed in Figure 3a. The PE particles appear to consist of agglomerates of spherical smaller particles, which show a relatively uniform diameter of 10–20 μm. This suggests that OS1, with a mean particle size of 134 μm, undergoes fragmentation upon applying shear forces during the MAO treatment in toluene suspension. Barron and co-workers[16] reported similar observations for the morphology of PE produced with *p*-hydroxybenzoic acid-modified nanoboehmites.

According to TEM investigations (cf. Figure 3b) of a typical polyethylene sample, the polyethylene matrix contains uniformly dispersed nanoboehmites of around 100 nm average diameter, which are assembled from boehmite crystallites of 10 nm average size. No larger agglomerates were detected. This provides experimental evidence for the very effective in situ formation of polyethylene nanocomposites resulting from the deagglomeration of arylsulfonic acid-modified boehmites during catalyst preparation and also during the subsequent polymerization.

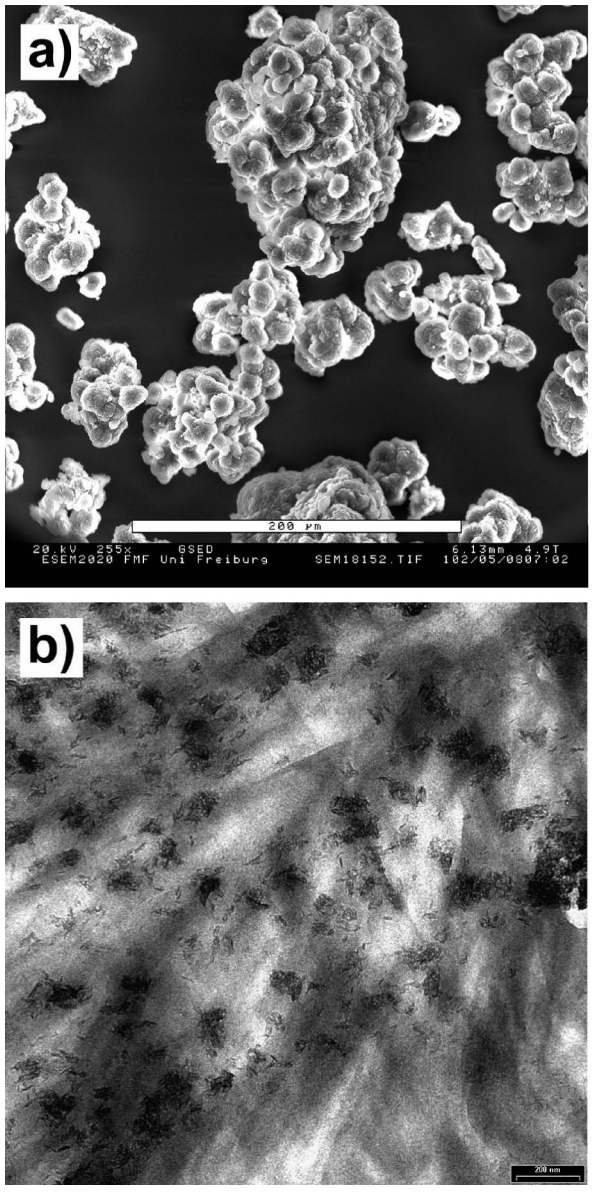

Figure 3. (a) ESEM image of PE particles obtained from Cp_2ZrCl_2/MAO/OS1 (run B4 in Table 3, scale bar = 200 μm) and (b) TEM image of the corresponding molded sample (scale bar = 200 nm).

Table 4. Bulk Density and Mean Particle Size of PE Obtained from the Catalyst Cp_2ZrCl_2/MAO/OS1 as a Function of Catalyst Preparation and Polymerization Temperature[a]

run	T_{react} [°C]	catalyst preparation	bulk density [g/L]	mean size (LS)[b] [μm]	mean size (CCD)[c] [μm]
B1	25	in situ immob	149	124	1785
B2	25	dry catalyst	235	59	744
B3	40	dry catalyst	249	74	176
B4	50	dry catalyst	326	80	144
B5	75	dry catalyst	346	86	208

[a] Polymerization conditions: cf. Table 3. [b] Measured by laser light scattering on Horiba LA-920 in dry dispersion mode. [c] Measured by CCD image analysis on Retsch Camsizer.

More detailed studies investigating the influence of various parameters on PE particle morphology were performed characterizing the bulk density and particle size distributions (PSDs) of PE particles obtained from runs B1−B5. PSDs were recorded by means of LS measurements on dry powder dispersions as well as by image analysis of CCD camera images of free-falling powder particles. As can be seen from Table 4 and Figure 4, the morphological properties of the PE particles obtained are dependent on catalyst preparation as well as on polymerization temperature. However, the general structures of the polymer particles are similar for all polymerization conditions. As described above, the polyethylene particles comprise agglomerates of much smaller, spherelike particles. The differences between the obtained polymer particles only relate to the size and shape of these agglomerates, while the sizes and shapes of the small, spherelike particles are very similar for all samples.

Polymerizations using the in situ immobilization technique (run B1, Table 4) and the feed of dried catalyst (run B2, Table 4) gave different morphologies and PSDs. With the in situ immobilized catalyst, the mean value of the PSD determined by light scattering is 124 μm, while the CCD image analysis gave a by far larger mean particle size of 1785 μm. The PSDs displayed in parts a and c of Figure 4 show that, with the dried catalyst, distinctly bimodal PSDs are obtained, although the PSDs differ by 1 order of magnitude depending on the characterization method. With the in situ prepared catalyst, however, rather monomodal distributions are obtained, showing only small shoulders at the lower end. These results probably can be ascribed to the presence of toluene in case of the in situ immobilization technique, whereas in the second case all toluene is removed to yield the dry catalyst. Apparently, the presence of toluene contained in the catalyst particles increases the tendency of the growing polymer particles to agglomerate.

It should be noted that the large difference between the two particle size measurements is very likely caused by the sample preparation and the specific features of the particle size

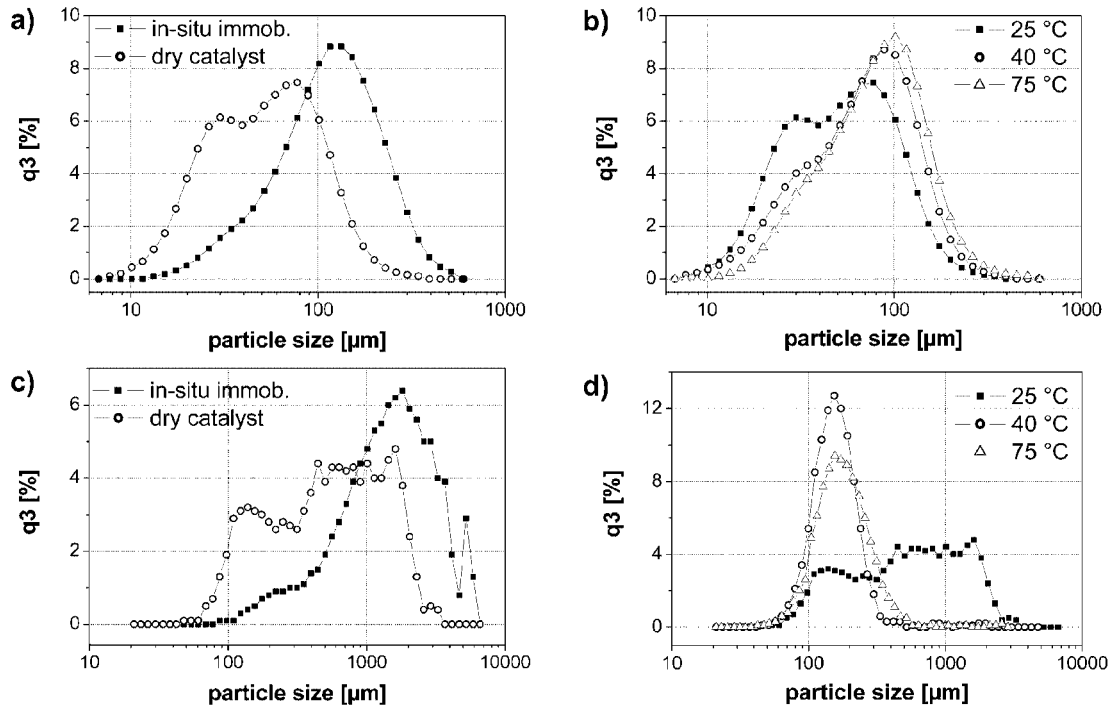

Figure 4. PSDs of PE particles produced by Cp_2ZrCl_2/MAO/OS1 with respect to (a and c) catalyst preparation technique (runs B1 and B2, Table 3) and (b and d) polymerization temperature (runs B2, B3, and B5, Table 3), as determined by (a and b) light scattering and (c and d) by CCD image analysis.

measurements. While the CCD camera image analysis of powder particles detects very large PE particles, shear forces of the air stream used in dry dispersion are likely to cause deagglomeration of the particles, thus accounting for the smaller PSDs measured by light scattering. Despite this experimental problem, both particle size measurements show the same trends with respect to the PE particle sizes, which are in good accord with those observed by ESEM.

Besides catalyst preparation, the polymerization temperature also affects the polymer particle morphology. Parts b and d of Figure 4 display polyethylenes obtained with the dried Cp_2ZrCl_2/MAO/OS1 catalyst at different temperatures. A shift toward larger polymer particles and monomodality is observed with increasing temperature when considering the light scattering measurements depicted in Figure 4b. The CCD image analysis measurements depicted in Figure 4d shows that the PSD of the polymer obtained at 25 °C is very broad and multimodal, pointing toward severe aggregation during polymerization. The PSDs of the polymers synthesized at higher temperatures, however, are narrow and clearly monomodal, with mean particle sizes around 200 μm. These PSDs are in acceptable accordance with those measured by light scattering. In addition, according to ESEM images, the polymer particles formed at higher temperatures are more spherical and dense. Consequently, the bulk density of those polymers is higher than that of polymers synthesized at lower temperature (cf. Table 4).

On-Line Monitoring of Polyethylene Particle Growth. A deeper understanding of the polyethylene particle formation and growth during polymerization was achieved by means of on-line monitoring using a laser back scattering method (focused laser beam reflectance measurement, "FBRM"). In contrast to most particle size measurement techniques, the FBRM probe can be inserted and run in the stirred polymerization reactor.[24–26] A rotating laser beam is reflected by any particle crossing the probe window, and the duration of the resulting signal is converted to the corresponding chord length (CL) of the particle.[24] The minimum measurement interval is 2 s, and during this time up to tens of thousands of CLs can be recorded. The resulting chord length distributions (CLDs) are square-weighted here for achieving a better visualization. The square-weighted CLDs are similar to the PSDs obtained from light scattering measurements, though not identical.[26] The measurement window of the FBRM probe applied in this study ranged from 1 to 1000 μm.

The FBRM on-line monitoring of polyethylene particle growth on Cp_2ZrCl_2/MAO/OS1 at 25 °C (run B1, Table 4) revealed that during the first 30 min relatively small particles with CLDs below 200 μm were formed and grew continuously (cf. Figure 5a). Only 10 minutes later, after 40 min of polymerization time, the CLD broadened almost instantaneously, then reaching up to 500 μm. Along with these changes, a sharp increase in the mean CL and a just as pronounced decrease in the number of counts was observed, as emerging from the trend analysis displayed in Figure 5b. Obviously, between 30 and 40 min of polymerization time, strong agglomeration took place, accounting for the formation of quite large agglomerates with very few particles smaller than 100 μm remaining. After 120 min, i.e., at the end of the polymerization, the CLD was monomodal again with a maximum around 300 μm. This final CLD is in striking contrast to the PSD of the isolated polymer particles obtained by off-line light scattering on dry particle dispersion with its maximum around 120 μm (cf. Figure 4a). Probably the air stream used for dry dispersion broke down a large portion of the agglomerates, resulting in a significant decrease of the measured particle sizes.

In the course of the ethylene polymerization at 40 °C using the dried Cp_2ZrCl_2/MAO/OS1 catalyst (run B3, Table 4), a continuous growth of the small starting particles was observed during the first 50 min (Figure 5c,d). Then a slight decrease in the total number of observed CLs accompanied by a significant increase of the mean CL was found, as shown in the trend analysis depicted in Figure 5d. These results refer to a minor aggregation process starting around 50 min after the polymerization was initiated.

In contrast, the polymerization at 75 °C exhibits a perfect growth of the polymer particles formed in the very first stages of the polymerization without any indication of agglomeration

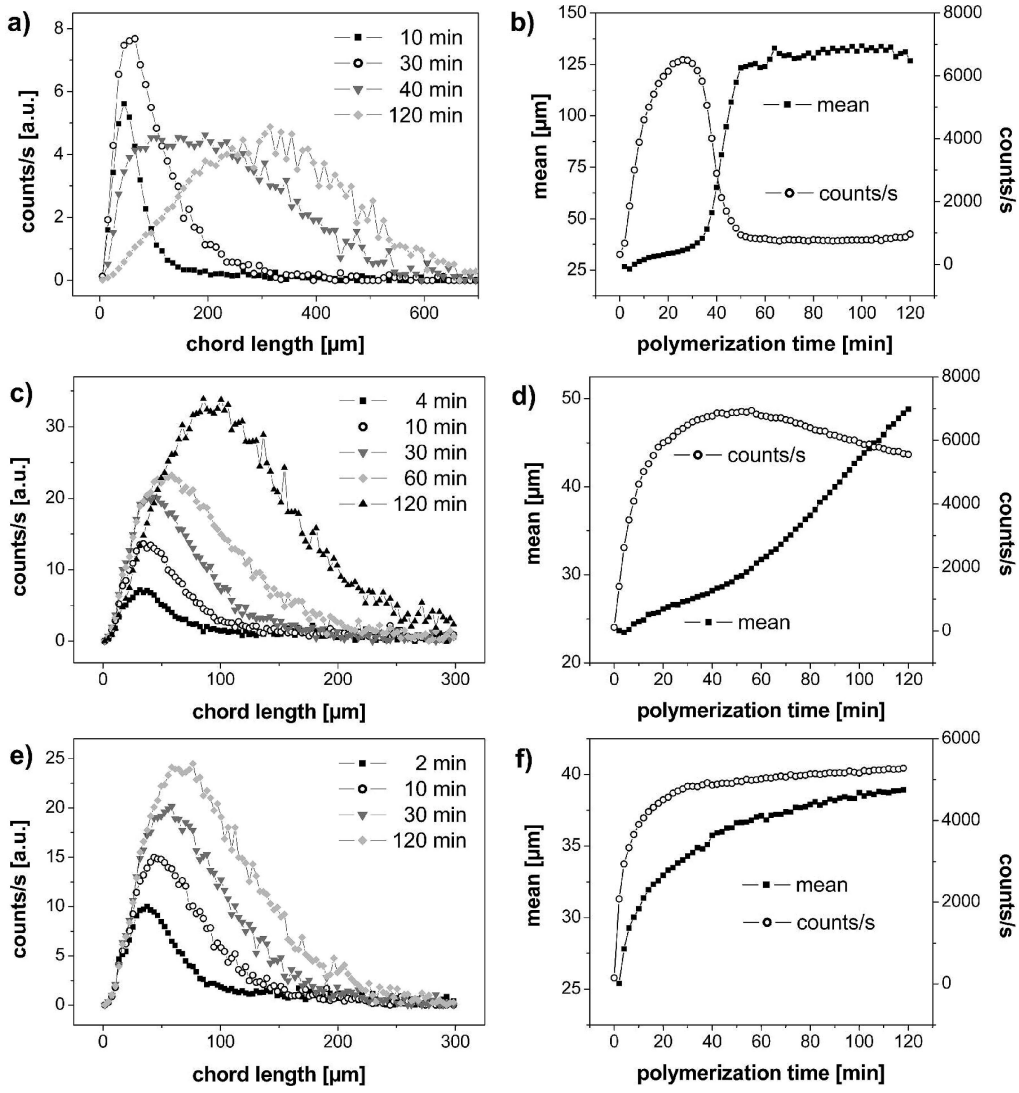

Figure 5. Selected square-weighted CLDs (left) and trends of mean CLDs and counts/s (right) for ethylene polymerizations (a and b) at 25 °C (run B1, Table 4), (c and d) at 40 °C (run B3), and (e and f) at 75 °C (run B5).

Scheme 3. Model for Polymer Particle Growth on Cp_2ZrCl_2/MAO/OS1 at 75 °C[a]

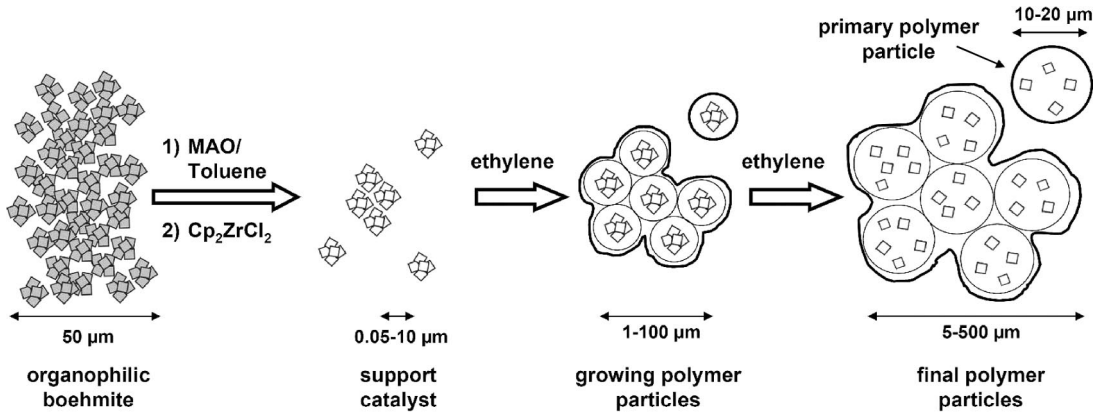

[a] Aggregation takes place only during very early stages but not during polymerization.

or fragmentation (Figure 5e,f). It should be noted here that the initial increase of the number of counts/s does not correspond to an increase in the total number of particles but is rather due to the fact that the probability of a particle to be tracked by the FBRM probe is proportional to its size.[24] The final CLD of the polymer produced at 75 °C has a somewhat lower maximum than that observed in the polymerization at 40 °C, though the off-line particle size measurements show quite similar PSDs for the polymer particles formed at 40 and 75 °C (cf. parts b and d of Figure 4). Again, this deviation is likely to result from fragmentation of the agglomerates in the air stream employed in the light scattering measurements.

The on-line measurements of size and concentration of the growing polymer particles clearly indicate that, at low temperatures, significant aggregation occurs during polymerization, whereas at 75 °C no agglomeration and fragmentation processes interfere with particle growth. Nevertheless, the polymer particles isolated from the polymerization at 75 °C also show similar morphology, which has been discussed in the section Off-Line Monitoring of Polyethylene Morphology (cf. Figure 3a). Obviously, agglomeration of the primary catalyst particles, which form the primary polymer particles, takes place before the start of the polymerization or in its very early stages. When polymerization progresses, aggregation of these growing agglomerates can occur as a function of polymerization temperature. Unfortunately, the size distribution of the supported catalyst cannot be determined unambiguously, as the FBRM technique is not sensitive enough to detect the small amount of nanometer-scaled catalyst particles in the reactor. Attempts to conduct off-line measurements failed because of the high sensitivity of MAO and active catalyst in the presence of traces of water and oxygen. When polymerization starts, the initially loose agglomerates are probably consolidated within the formed polyethylene. This mechanistic hypothesis is depicted in Scheme 3, which illustrates particle formation during ethylene polymerization for run B5 at 75 °C, in which no indication for aggregation of the growing polymer particles was given by the FBRM on-line monitoring. In the first step, the nanometer-scaled organophilic boehmites were dispersed in the solvent due to shear-induced deagglomeration of the organoboehmites. The obtained nanometer-scaled agglomerates of the boehmite crystallites of 10 nm average size form the active supports which immobilize MAO and metallocene. Upon initiation of polymerization, such nanoparticles grow to form polyethylene particles which agglomerate to larger particles. The catalyst formation and boehmite agglomeration and deagglomeration is readily controlled by the surface functionalities of the boehmites. This dispersion process leads to polyethylene containing uniformly dispersed nanometer-scale aggregates of the boehmite crystallites.

These observations are in good agreement with earlier reports by Klapper, Müllen, and co-workers on catalysts supported on organic polystyrene nanoparticles functionalized with polyethers such as PEO[10] and PPO.[11,12] These polyether chains on the surface were used for immobilization of MAO and metallocene accompanied by agglomeration of the primary catalyst nanoparticles to much larger secondary particles. In the course of ethylene polymerization and ethylene/1-olefin copolymerization, these secondary particles deaggregated and led to the homogeneous distribution of the organic support nanoparticles within the polymer. In conclusion, arylsulfonic acid-modified boehmites are attractive components to produce nanometer-scaled organic/inorganic nanohybrid catalysts.

Conclusions

Arylsulfonic acid-modified boehmites are very effective supports for MAO and the in situ activation of ethylene polymerization. The arylsulfonic acid modification of boehmite increases the amount of MAO that can be immobilized on the support by a factor of 4−8 with respect to unmodified boehmite. MAO uptake depends on the type of arylsulfonic acid employed. This MAO uptake reflects the strong Lewis acid/Lewis base interactions between MAO and surface sulfonate groups of the modified boehmites. In addition, according to NMR investigations, the reaction of surface arylsulfonates with aluminum alkyls produces methylarylsulfones which are Lewis bases playing an important role in MAO and metallocene immobilization. Moreover, the organophilic boehmite modification enables the deagglomeration of boehmite to form nanometer-sized boehmite particles which are composed of small assemblies of the primary boehmite nanocrystallites. Such nanometer-scaled boehmite assemblies are very effective supports for MAO and transition-metal complexes. The growth and the morphology of polyethylene particles is dependent upon the organophilic boehmite modification and the reaction conditions such as polymerization temperature. The on-line monitoring of polyethylene particle growth by means of laser back scattering is an attractive route to monitor particle growth in a stirred reactor. The nanoparticle assembly and the controlled growth of polyethylene particles produce micrometer-scaled polymer particles and prevent the severe reactor fouling typical for the corresponding homogeneous metallocene catalysts. Tailor-made organoboehmites are very versatile with respect to supporting various main-group metal alkyls and metallocene as well as postmetallocene catalysts. The in situ formation of well-dispersed nanoboehmites during polymerization represents an attractive route to polyolefin nanocomposites with uniform nanometer-scaled boehmite particle dispersions.

Acknowledgment. The authors gratefully acknowledge the financial support by BMBF (Project Nos. 03C0354A and 03C0354B), as part of a close collaboration with Basell Polyolefine GmbH, and the Fonds der Chemischen Industrie. We also thank Mr. Olaf Torno form Sasol Germany GmbH, Hamburg, for supplying us with arylsulfonic acid-modified boehmites.

References and Notes

(1) Hlatky, G. G. *Chem. Rev.* **2000**, *100*, 1347–1376.
(2) Severn, J. R.; Chadwick, J. C.; Duchateau, R.; Friederichs, N. *Chem. Rev.* **2005**, *105*, 4073–4147.
(3) Sinn, H.; Kaminsky, W.; Vollmer, H. J.; Woldt, R. *Angew. Chem., Int. Ed. Engl.* **1980**, *19*, 390–392.
(4) Sinn, H.; Kaminsky, W. *Adv. Organomet. Chem.* **1980**, *18*, 99.
(5) Wild, F.; Zsolnai, L.; Huttner, G.; Brintzinger, H. H. *J. Organomet. Chem.* **1982**, *232*, 233–247.
(6) Kaminsky, W.; Kulper, K.; Brintzinger, H. H.; Wild, F. *Angew. Chem., Int. Ed. Engl.* **1985**, *24*, 507–508.
(7) Eberhardt, A. M.; Ferreira, M. L.; Damiani, D. E. *Polym. Eng. Sci.* **2001**, *41*, 946–954.
(8) Lee, D. H.; Yoon, K. B.; Huh, W. S. *Macromol. Symp.* **1995**, *97*, 185–193.
(9) Lee, D. H.; Yoon, K. B. *Macromol. Rapid Commun.* **1994**, *15*, 841–843.
(10) Koch, M.; Falcou, A.; Nenov, N.; Klapper, M.; Müllen, K. *Macromol. Rapid Commun.* **2001**, *22*, 1455–1462.
(11) Jang, Y. J.; Nenov, N.; Klapper, M.; Müllen, K. *Polym. Bull.* **2003**, *50*, 343–350.
(12) Jang, Y. J.; Nenov, N.; Klapper, M.; Müllen, K. *Polym. Bull.* **2003**, *50*, 351–358.
(13) Kissin, Y. V. *J. Polym. Sci., Part A: Polym. Chem.* **2005**, *43*, 689–692.
(14) Harrison, D.; Coulter, I. M.; Wang, S.; Nistala, S.; Kuntz, B. A.; Pigeon, M.; Tian, J.; Collins, S. *J. Mol. Catal. A: Chem.* **1998**, *128*, 65–77.
(15) Marques, M. D. V.; De Alcantara, M. *J. Polym. Sci., Part A: Polym. Chem.* **2004**, *42*, 9–21.
(16) Obrey, S. J.; Barron, A. R. *Macromolecules* **2002**, *35*, 1499–1503.
(17) Leach, B. E.; Decker, L. B. U.S. Patent 4,676,928 (Vista Chemical Company), 1987.
(18) Hurlburt, P. K.; Plummer, D. T. U.S. Patent 6,224,846 (Condea Vista Company), **2001**.
(19) Alamo, R. G.; Mandelkern, L. *Macromolecules* **1989**, *22*, 1273–1277.
(20) Chu, K. J.; Soares, J. B. P.; Penlidis, A. *J. Polym. Sci., Part A: Polym. Chem.* **2000**, *38*, 1803–1810.
(21) Chu, K. J.; Soares, J. B. P.; Penlidis, A. *J. Polym. Sci., Part A: Polym. Chem.* **2000**, *38*, 462–468.
(22) do Couto, P. A.; Nele, M.; Coutinho, F. M. B. *Eur. Polym. J.* **2002**, *38*, 1471–1476.
(23) SDBSWeb. http://www.aist.go.jp/RIODB/SDBS/ (National Institute of Advanced Industrial Science and Technology, 28.08. **2007**).
(24) Ruf, A.; Worlitschek, J.; Mazzotti, M. *Part. Part. Syst. Charact.* **2000**, *17*, 167–179.
(25) Dowding, P. J.; Goodwin, J. W.; Vincent, B. *Colloid Surf., A:* **2001**, *192*, 5–13.
(26) Heath, A. R.; Fawell, P. D.; Bahri, P. A.; Swift, J. D. *Part. Part. Syst. Charact.* **2002**, *19*, 84–95.

MA702623E